This is a repository copy of *ATP-dependent dynamic protein aggregation regulates bacterial dormancy depth critical for antibiotic tolerance*.

White Rose Research Online URL for this paper:
https://eprints.whiterose.ac.uk/id/eprint/138082/

Version: Accepted Version

Article:

ATP-dependent dynamic protein aggregation regulates bacterial dormancy depth critical for antibiotic tolerance

Yingying Pu[1,#], Yingxing Li[1,#], Xin Jin[1,#], Tian Tian[1,#], Qi Ma[1], Ziyi Zhao[1], Ssu-yuan Lin[2], Zhanghua Chen[1], Binghui Li[3], Guang Yao[4], Mark C. Leake[5,6], Chien-Jung Lo[2], Fan Bai[1,*]

1. Biomedical Pioneering Innovation Center (BIOPIC), School of Life Sciences, Peking University, Beijing 100871, China.
2. Department of Physics and Graduate Institute of Biophysics, National Central University, Jhong-Li, Taoyuan 32001, Republic of China.
3. Department of Biochemistry and Molecular Biology, Capital Medical University, Beijing, Beijing 100069, China.
4. Department of Molecular and Cellular Biology, University of Arizona, Tucson, AZ, 85721, USA
5. Department of Physics, University of York, York YO10, United Kingdom
6. Department of Biology, University of York, York YO10, United Kingdom

# These authors contributed equally to this work

* Lead contact, corresponding author: Fan Bai, fbai@pku.edu.cn

SUMMARY

Cell dormancy is a widespread mechanism used by bacteria to evade environmental threats including antibiotics. Here we monitored bacterial antibiotic tolerance and regrowth at the single-cell level and found that each individual survival cell shows different 'dormancy depth', which in return regulates the lag time for cell resuscitation after removal of antibiotic. We further established that protein aggresome - a collection of endogenous protein aggregates - is an important indicator of bacterial dormancy depth, whose formation is promoted by decreased cellular ATP level. For cells to leave the

dormant state and resuscitate, clearance of protein aggresome and recovery of proteostasis are required. We revealed the ability to recruit functional DnaK-ClpB machineries, which facilitate protein disaggregation in an ATP-dependent manner, determines the lag time for bacterial regrowth. Better understanding of the key factors regulating bacterial regrowth after surviving antibiotic attack could lead to new therapeutic strategies for combating bacterial antibiotic tolerance.

Introduction

The ability of some bacteria within a population to tolerate antibiotic treatment is often attributed to prolonged bacterial infection, such as tuberculosis and cystic fibrosis associated lung infections (Boucher, 2001; Chao and Rubin, 2010). Unlike antibiotic resistance, which generally results from genetic mutations or plasmid transfer (Toprak et al., 2011), antibiotic tolerance usually refers to the phenomenon that a subgroup of cells can survive high-dose antibiotic treatment as a result of phenotypic heterogeneity (Fridman et al., 2014; Pu et al., 2016). Such non-genetic individuality maximizes the survival probability for a bacterial population in a rapidly changing environment, as different phenotypes may gain higher fitness for different stresses.

Previous studies mainly associated antibiotic tolerance with cell dormancy by hypothesizing that the lethal effects of antibiotics are disabled due to the extremely slow metabolic and proliferation rates in dormant bacteria (Balaban et al., 2004). Molecular mechanisms leading to cell dormancy in bacteria are usually redundant, including the toxin-antitoxin (TA) modules (Balaban et al., 2004), stringent response (Harshman and Yamazaki, 1971), oxidative stress response pathways (Vega et al., 2012), and global regulators leading to slow metabolism (Hansen et al., 2008). Since the discovery of high-persistence mutants that possess nucleotide replacement in *hipA* gene (a toxin) (Moyed and Bertrand, 1983), numerous studies have investigated the role of TA modules in bacterial drug tolerance. Stringent response is another well-studied mechanism involved in bacterial cell dormancy. In a shortage of amino

acid, stringent response is evoked through the synthesis of small molecule alarmones; (p)ppGpp is a typical alarmone that is responsible for sensing environmental stresses and thereby inducing downstream pathways to drive bacteria into a dormant state (Kaspy et al. 2013). In dormant cell formation, distinct molecular mechanisms may work simultaneously and cooperatively. However, as dormant cells only comprise a small fraction of a bacterial population, traditional methods based on population experiments, which are prone to mask individual heterogeneity and system complexity, are inadequate. Recently, through the use of single cell technologies in-depth investigation of cell dormancy linked to drug tolerance is possible, enabling exploration of new cellular mechanisms.

So far, many existing researches mainly focus on how bacterial cells are driven into a dormant state and evade antibiotic attack. However, less is known about how surviving bacteria subsequently escape from the dormant state and resuscitate, which plays an equally important role in disease recurrence. In this study, we have combined *in vivo* fluorescence imaging with proteome-wide mass spectrometry to explore the role of putative protein aggresomes in regulating bacterial drug tolerance. We postulate that the degree to which drug-tolerant cells are dormant can be measured by a parameter we term the 'dormancy depth'. Persister cells are considered to be in shallow dormancy depth, while viable but non-culturable cells (VBNC cells) are in a deeper dormancy. Furthermore, we find that the dormancy depth in individual cells is closely correlated with the appearance of a novel cellular feature – dark foci caused by protein aggresomes. Finally, we explore the important biological processes involved in the production and clearance of these cellular aggresomes and their specific contributions to bacterial drug tolerance. Our work sheds new light on how ATP-dependent dynamic protein aggregation regulates cellular dormancy and resuscitation, the fine control of which enables some bacteria to survive antibiotic attack, and may present new strategies for the development of new therapies to circumvent bacterial antibiotic tolerance.

Results

Drug tolerant cells are highly heterogeneous in their ability to recover from the dormant state

In our experiment, an overnight culture of *Escherichia coli* was exposed to a high concentration of ampicillin (150 μg ml^{-1}) treatment, 15 times the minimum inhibitory concentration (MIC). We monitored the antibiotic killing process in real time using high-throughput light microscopy, which enabled observation of the same group of cells for extended periods. Most cells were killed by lysis, however, a small group of cells, typically composed of non-proliferative dormant cells, survived 6 hours of antibiotic treatment. We continued to observe the resuscitation course of these survival cells after removing antibiotics. We observed that some cells resumed growth very soon ($T_{regrowth}$<12 hours), meeting the classic definition of persisters (referred to as persister-fast-recovery, persister-FR, Figure 1A top, Video S1). In contrast, a considerable proportion of surviving cells remained in a dormant state showing no signs of growth. Extension of the observation period revealed that some of these dormant cells escaped from dormancy and started to proliferate (12 hours<$T_{regrowth}$<40 hours) (referred to as persister-slow-recovery, persister-SR, Figure 1A middle, Video S2). The remainder of the surviving cells remained dormant even after three days of observation (viable but non-culturable cells, VBNC cells (Ayrapetyan et al., 2015), Figure 1A bottom, from which dead cells were excluded by propidium iodide staining (Figure S1A). This result was reproducible at a population level. After we treated a bacterial population with 150 μg ml^{-1} of ampicillin for 5 hours in a conical tube, we cultured the survival cells on fresh LB agar plates. Alongside colonies that were visible after one day more colonies (an increase of approximately 25%) gradually emerged over subsequent days (Figure 1C). These results reveal that drug tolerant cells are highly heterogeneous in their ability to recover from the dormant state. In other words, drug tolerant cells show a broad distribution of lag times (Balaban et al., 2004).

Based on these observations, we postulated that the degree to which drug tolerant cells are dormant can be measured by a parameter we term 'dormancy depth'. Cells trapped in a dormant state are protected from antibiotic killing, but after removal of

the antibiotic the trapped cells are able to escape from their dormant state and re-enter the active cell cycle at a rate determined by the dormancy depth. We further hypothesized that bacterial dormancy is not a single homogeneous state but displays a dormancy depth continuum. Persister-FR cells are trapped at a shallow dormancy depth and it is therefore easy for them to escape and resume growth (Figure 1B); Viable but nonculturable (VBNC) cells, residing at deeper dormancy depths, have too large a barrier to overcome in order to escape, and thus cannot initiate resuscitation (Figure 1B); persister-SR cells are in an intermediate region between these two extremes.

The dormancy depth appears to be conceptually similar to the 'quiescence depth' in eukaryotic cells, which can be induced by serum starvation (Wang et al., 2017). To probe this similarity, we tested whether bacterial dormancy depth can be modulated by culturing a bacterial sample for longer in stationary phase at 37°C. As seen in Figure 1D, the number of dormant cells, defined as cells non-proliferating for at least 6 hours in fresh medium when observed under a microscope, increased with culture time under stationary phase indicating that prolonged nutrient depletion resulting from increased culturing time drives more cells into deeper dormancy. We also performed antibiotic killing and persister counting in parallel for bacterial populations cultured for different time periods. In contrast to the dormant cell ratio (proportion of dormant cells in the population), the persister cell ratio (proportion of persister cells in the population) initially increased steadily, peaked after 24 hours of incubation, then decreased gradually, indicating that more dormant cells have become VBNC cells (Figure 1E and S1B-S1E, persister cells were validated to be phenotypically tolerant to antibiotics using MIC measurement and growth curve calibration, Figure S1F). These results reveal that bacterial dormancy depth can be modulated by the culturing conditions. In addition, in accordance with our model, the persister cell ratio can be optimized by increasing the number of dormant cells, whilst avoiding driving them into deep dormancy depths. The same phenomenon can be reproduced with other types of antibiotics – ciprofloxacin, nalidixic acid, carbenicillin and amoxicillin (Figure S1B-S1E). Combining these results, we describe dormancy as a

heterogeneous physiology state with differing depths. As dormancy shields cells from antibiotic killing effects, dormancy depth regulates whether and when (the lag time) survival cells resuscitate.
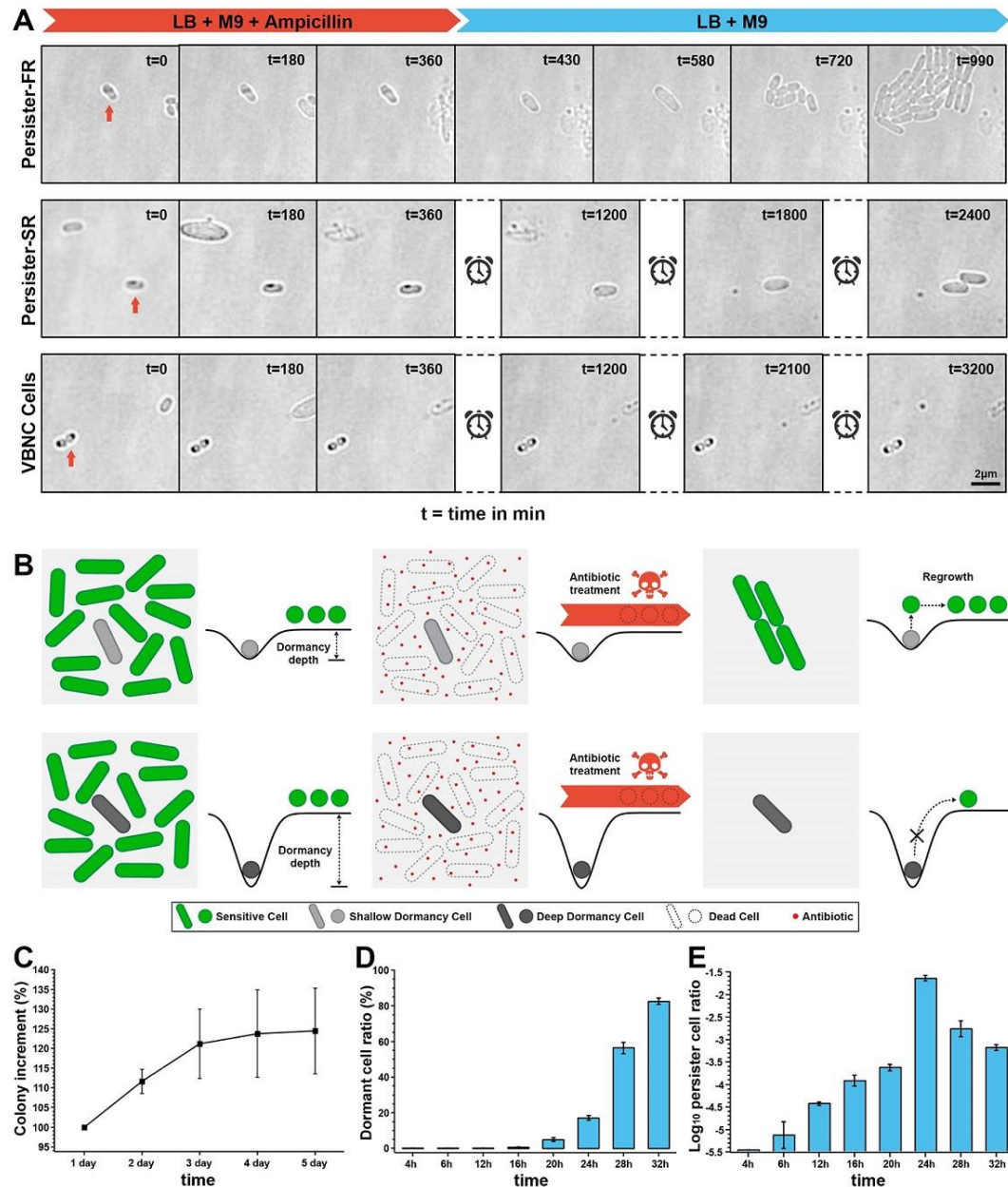
Figure 1. Drug tolerant cells are highly heterogeneous in their ability to recover from the dormant state.

(A) Time-lapse images of persister-FR (upper), persister-SR (middle) and VBNC (lower) cells during antibiotic killing   and subsequent resuscitation of survival cells (replacing the killing medium with fresh growth medium, Video S1). Persister-FR cells resuscitate very soon after removal of antibiotic whereas persister-SR cells resuscitate slowly. VBNC cells survive antibiotic

treatment but show no sign of resuscitation in the 3 days after removal of antibiotic. Scale bar, 2 μm; t=time (min).

(B) Model summarising how bacterial dormancy depth regulates antibiotic tolerance and regrowth.

(C) Number of CFU persister cells present at indicated culture time after removal of antibiotic.

(D) Ratio of dormant cells as function of culture time from inoculation. Dormant cells are defined as cells non-proliferating for at least 6 hours on fresh agarose when observed under a microscope.

(E) Frequency of persister formation as function of culture time from inoculation, determined by antibiotic susceptibility measurement.

The bars indicate mean of at least three independent experiments; error bar indicates STDEV.

See also Figure S1and S6.

Aggresome correlates with bacterial dormancy depth

We then investigated what phenotypic trait can indicate the bacterial 'dormancy depth' at a single-cell level. Under brightfield microscopy observations, we noticed that a novel phenotypic feature - dark foci - often accompanied dormant cells but was not present in actively growing cells (red arrows Figure 1A). Normally one or two dark foci were observable per dormant cell, predominantly at the cell poles, but also in mid- or quarter- cell positions. We suspected that these dark foci would be protein aggresomes - a collection of protein aggregates formed when intracellular proteostasis is disrupted. To test this hypothesis, we labelled IbpA, a small molecular chaperone that tightly associates with bacterial protein aggregates (Lindner et al., 2008; Ungelenk et al., 2016), with enhanced green fluorescent protein (EGFP). As shown in Figure 2A, IbpA-EGFP colocalised with the dark foci visible in brightfield implying that dark foci are composed of protein aggregates.

Consistent with this observation, when dormancy depth was increased by culturing cells for longer at stationary phase the fraction of insoluble protein in the cell also increased (Figure 2B). Total protein mass-spectrometric analysis of 16 hours, 24 hours and 32 hours cultures identified 399, 907 and 904 types of insoluble protein respectively (Table S1). These insoluble proteins included numerous essential and non-essential proteins involved in a range of important biological processes (Figure 2C and S2A-S2C), consistent with the hypothesis that dark foci are aggresomes which result from an extensive proteome-wide aggregation process. This is a plausible explanation for why these cells fail to maintain regular metabolism and enter a

dormant state, since aggresomes partition off many proteins which are vital for cellular function. We further compared the types of proteins included in the aggresomes at their early stage of formation (after 16 hours culturing) to that at their late stage of formation (after 32 hours culturing) (Figure S2A). Kyoto Encyclopedia of Genes and Genomes (KEGG) pathway analysis revealed that most proteins aggregated at the early stage are ribosome proteins, and proteins associated with carbon metabolism and oxidative phosphorylation, suggesting that pathways related to energy generation and protein production are the first to be shut down during starvation (Figure S2B). Then, a significant enrichment of DNA replication and repair related proteins was observed in the late stage, suggesting that DNA replication is shut down after a prolonged time of starvation (Figure S2C). Although the number of insoluble protein types in the 24 and 32 hours cultures was similar, analysis revealed that for almost all protein types the abundance of insoluble fraction increases as a function of time (Figure 2C). These results suggest that the shutdown of different biological processes may follow some level of sequential order. Also, that closure of a particular biological pathway is gradual during starvation. Taken together, these observations hint towards the existence of cell dormancy depth.

To further confirm that the proteins in the aggresome are aggregated, we identified two proteins, Lon and HslU, which accumulated gradually in the insoluble protein fraction with increased culture time (Table S1). In cells sensitive to antibiotic these two proteins exhibit a homogeneous distribution through the cytoplasm (Winkler et al., 2010). We labelled these proteins with TC-FlAsH, a marker whose fluorescence increases more than 3-fold when aggregation occurs (Ignatova and Gierasch, 2004). As expected, bright Lon-TC-FlAsH and HslU-TC-FlAsH foci colocalised with dark foci in the brightfield image (Figure 2A).

Next, we investigated how bacterial dormancy depth associates with the appearance of protein aggresome. According to cell responses to antibiotic treatment we divided the bacterial cell population into four subgroups: sensitive, persister-FR, persister-SR and VBNC cells characterized by a deepening dormancy depth

(Figure 1A). Within the four subgroups the proportion of cells containing one or more protein aggresomes, either labelled with IbpA-EGFP, Lon-TC-FlAsH or HslU-TC-FlAsH, increased with dormancy depth (Figure 2D) indicating a strong correlation between dormancy depth and the presence of protein aggresomes. The reason that IbpA is more sensitive to protein aggregates may come from its non-specificity; IbpA associates with most unfolded proteins whereas TC-FlAsH labels only one.
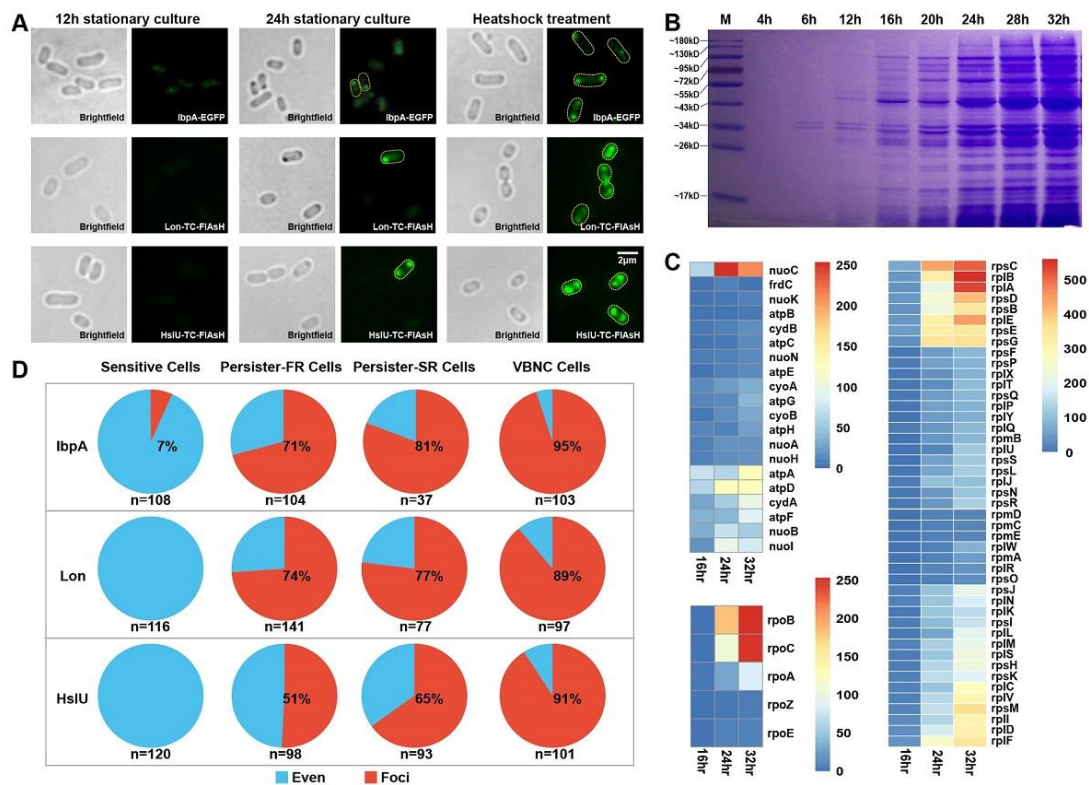

Figure 2. Aggresome correlates with bacterial dormancy depth.

(A) Brightfield and fluorescence images of cells showing protein aggresome are induced in prolonged stationary phase or by heat shock (12-hour culture treated by heatshock at 48°C for one hour). Protein aggregates labelled by IbpA :: EGFP (upper), Lon :: TC-FlAsH (middle) and HslU :: TC-FlAsH (lower). The cells were stained with FlAsH for 50 minutes and washed with fresh PBS buffer before heatshock treatment (Scale bar, 2 μm).

(B) Fraction of endogenous insoluble protein in the cultures from indicated culture time.

(C) Heatmaps showing the insoluble proteins of 16 hours, 24 hours, 32 hours cultures that are involved in several important biological processes, including oxidative phosphorylation, transcription and translation. Heatmap scale indicates protein abundance.

(D) Percentage of cells with protein aggresome in different cell subgroups of 24 hours culture (sensitive cells, persister-FR cells, persister-SR cells and VBNC cells) using the three fluorescent labelling methods.

See also Table S1, Figure S2.

Formation of aggresomes facilitates bacterial cell dormancy

To test if protein aggresomes can cause cell dormancy we induced massive endogenous protein aggregation in cells by heat shock (Wallace et al., 2015) (Figure 3A). Mass spectrometry data confirmed that the relative type and abundance of insoluble proteins produced by heat shock is similar to that generated by prolonged culturing of bacterial samples (Figure 3B). We found that the fraction of insoluble protein increased with increasing heat shock temperature. The corresponding dormant cell ratio also increased with cellular protein aggregation accumulation (Figure 3C and S3A). In contrast, when heat shock temperature was below 48°C the persister ratio of the population increased with temperature, but above this temperature the persister ratio decreased gradually (Figure 3D and S3B), again suggesting that survival cells with deeper dormancy depth are more difficult to resuscitate. Furthermore, we tried to induce protein aggresome formation by adding streptomycin (Lindner, *et al.*, 2008) or hydrogen peroxide (Mirzaei & Regnier, 2008) (Figure S3C). The dormant cell ratio increased similarly when protein aggregation occurred (Figure S3D).

Next, we examined whether prevention of aggresome formation would stop a cell from sliding into a deep dormancy state in stationary phase. As newly synthesized polypeptides are required for initiation of protein aggregation (Hartl et al., 2011; Zhou et al., 2014), inhibition of translation would prevent aggresome formation and therefore attenuate cell dormancy. To test this hypothesis, we treated cells with chloramphenicol, a drug that can inhibit protein synthesis through preventing protein chain elongation (Siibak et al., 2009), before dormant cell ratio analysis. As illustrated in Figure 3E, cells cultured in LB for 16 hours at 37°C were taken out and split into

two tubes, one containing 25 μg/ml chloramphenicol and the other without and incubated further. Next, a fraction of cells was taken out at indicated time point and chloramphenicol was washed away for dormant cell ratio analysis (Figure 3E). Chloramphenicol treated cells showed no detectable sign of dark foci under brightfield microscopy observation, even when the total culture time reached 32 hours, indicating that aggresome formation does not occur in translation-inhibited cells (Figure 3F). Consistently, the dormant cell ratio in chloramphenicol-treated cells (Figure 3G and S3E, red bars) was significantly lower when compared to the control counterpart (Figure 3G and S3E, blue bars), confirming that suppression of aggresome formation can prevent cell dormancy effectively. Taken together these results reinforce our dormancy depth model and suggest that the formation of cellular protein aggresomes facilitates cell dormancy.
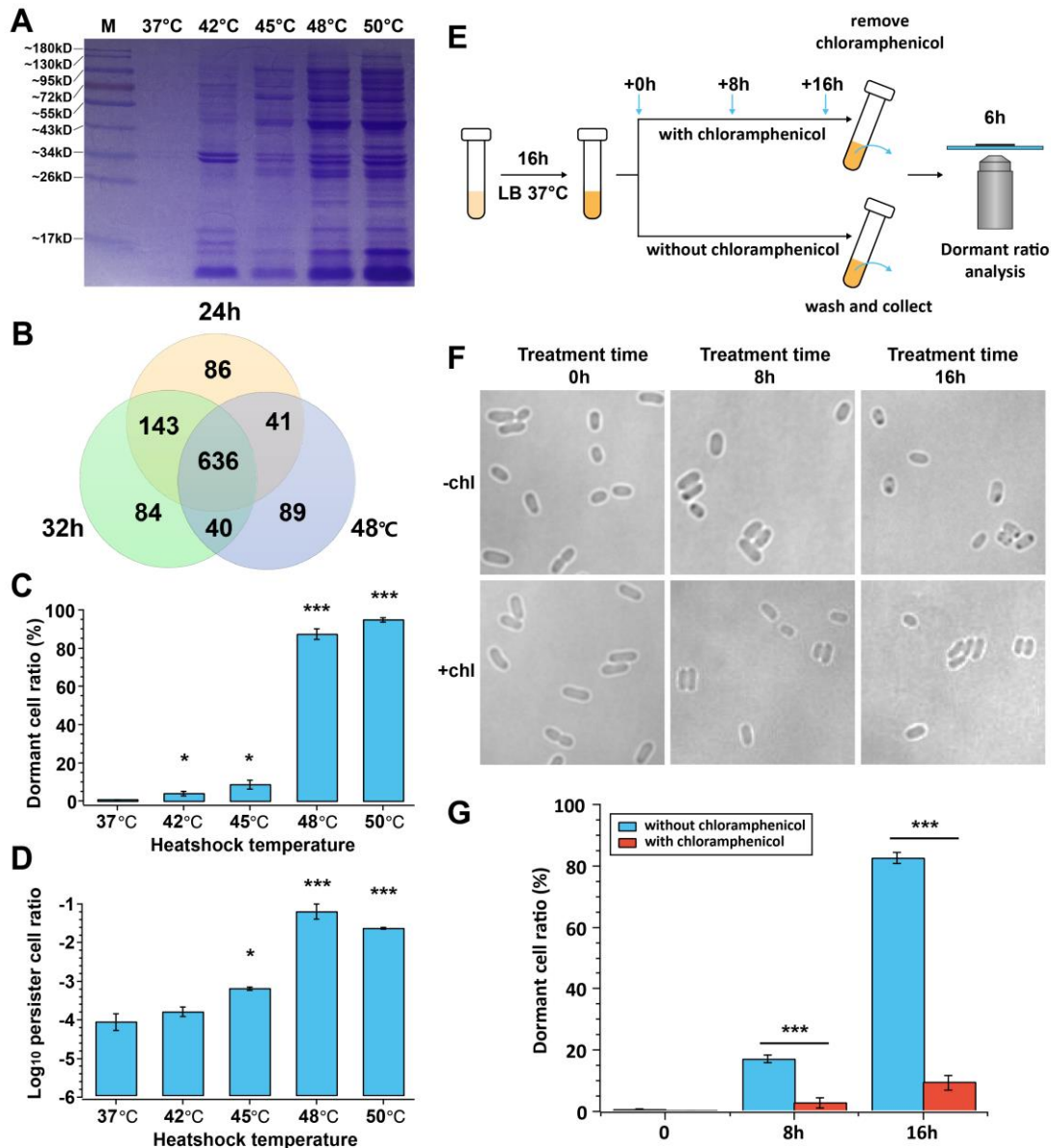
Figure 3. Formation of aggresome facilitates bacterial cell dormancy.

(A) Fraction of endogenous insoluble protein in the cultures treated at different temperatures.

(B) Venn diagram showing the insoluble protein overlap in 24 hours and 32 hours cultures and heat shock treatment sample (produced by treating a 16 hours culture for 1 hour at 48°C). For all three conditions approximately 2/3 of the insoluble proteins were identical.

(C) Proportion of dormant cells (the 'dormant cell ratio') after heat shock treatment. Dormant cells are defined as cells which do not proliferating for at least 6 hours on fresh agarose when observed under a light microscope.

(D) Frequency of persister formation after heat shock treatment, determined by antibiotic susceptibility measurement .

(E) Experimental design for preventing cells from dormancy by inhibition of aggresome formation. 16 hours cultured cells at 37°C were took out and split into two tubes, one added with 25 μg/ml chloramphenicol and the other without. Then the tubes were returned to the incubator for further culture. Next, a fraction of cells were taken out at indicated time point and washed away

chloramphenicol for dormant cell ratio analysis.

(F) Cell morphology observed under a bright field microscope. The 16 hours cultured cells were treated with or without chloramphenicol for 0 hour, 8 hours and 16 hours, respectively.

(G) Dormant cell ratio of cells with or without chloramphenicol treatment for 0 hour, 8 hours and 16 hours, respectively. Dormant cells are defined as cells non-proliferating for at least 6 hours on fresh agarose when observed under a microscope.

The bars indicate mean of at least three independent experiments; error bar indicates STDEV (*p value < 0.05; **p value < 0.005; ***p value < 0.0005).

See also Figure S3 and S6.

Aggresome formation accompanies a small but statistically significant shift in intracellular pH

We then sought to understand why aggresomes form in bacterial cells after long time stationary phase culturing. In the established yeast stress adaption model (Munder et al., 2016), nutrient scarcity causes cellular ATP depletion and a drop in cytosolic pH, which in turn promotes macromolecule granule formation and cytoplasmic solidification, therefore enhancing cell dormancy. Inspired by these observations from eukaryotes, we investigated the intracellular pH changes using pHluorin (Miesenbock et al., 1998) which is a genetically encoded ratiometric fluorescent sensor that can indicate pH changes at a single cell level (Figure S4A). We found that along with increased culture time, the intracellular pH of bacterial cells decreased gradually (Figure 4A). The average intracellular pH in the exponential growth phase (3 hours) is 8.08 ± 0.31, which decreases to 7.57 ± 0.25 in cells after 6 hours culturing, then to 7.14 ± 0.23 in cells after 32 hours culturing. We further investigated whether the cytoplasmic pH differs in cells with aggresomes present compared to those in which aggresomes were absent. Interestingly, we found that cells with dark foci in brightfield image have lower pH than the cells without dark foci in a bacterial population cultured for 32 hours ($\Delta pH = 0.24$, p value < 0.0005), indicating a correlation between acidic cytoplasm and aggresome formation (Figure 4B).

We then tested whether a drop in intracellular pH is causal to promote protein aggresome formation. We added 40 mM potassium benzoate and 40 mM methylamine hydrochloride to collapse the difference between external pH and internal pH such that the pH of the medium and the cytoplasmic are the same (Martinez, et al. 2012). Then we modulated cytoplasmic pH through adjustment of the pH of the growth medium (Figure S4B). Although the intracellular pH of the cells had been adjusted to be acidic (pH = 6.92), after additional incubation of 4 hours, we failed to observe aggresome formation. These results suggest that in nutrient depleted cells, aggresome formation accompanies intracellular pH drop, however, an acidic cytoplasm is not the direct or singular reason that causes protein aggresome formation in bacterial cells.
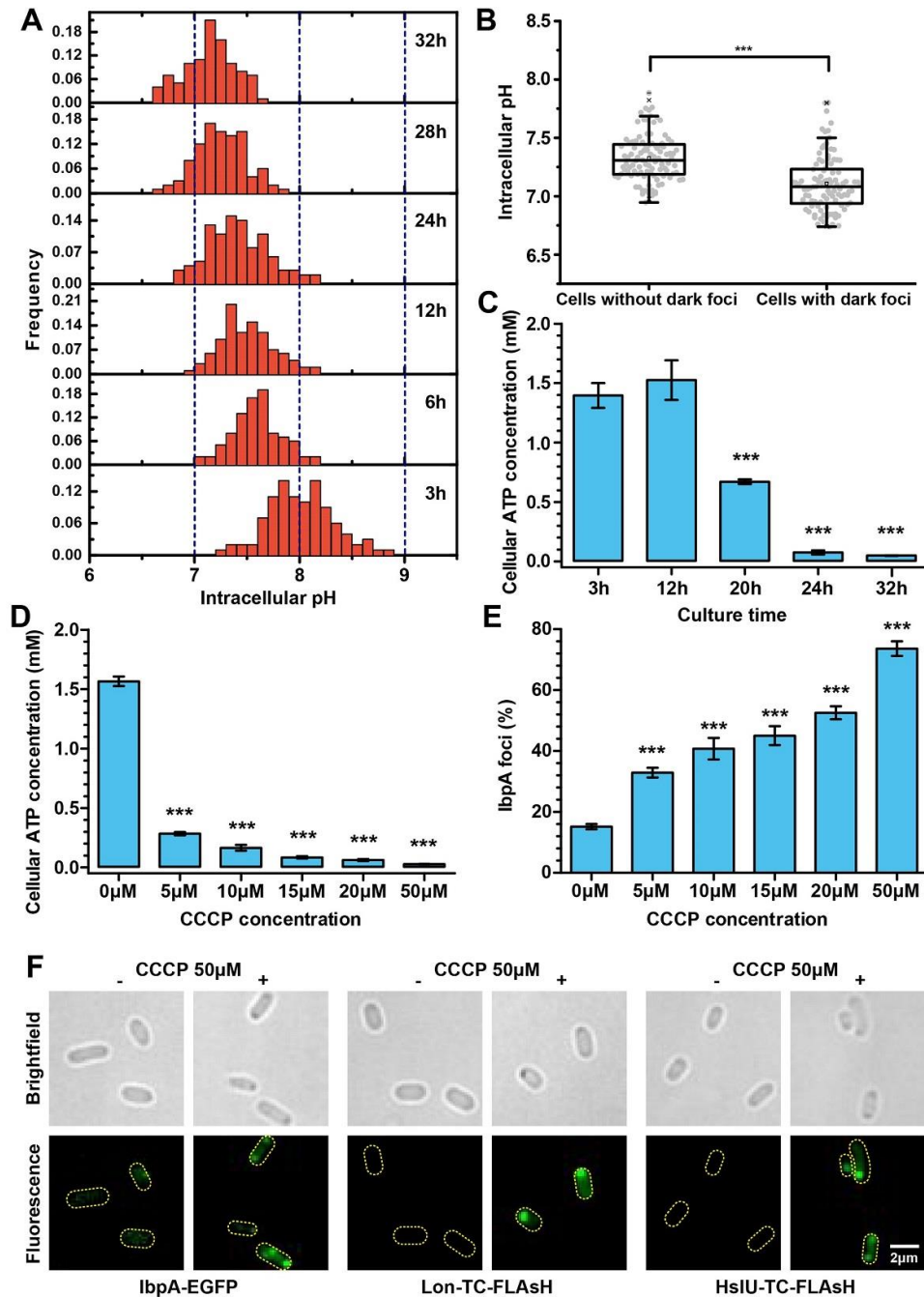
Figure 4. Intracellular ATP depletion promotes aggresome formation.

(A) Histogram of intracellular pH of cells with different culture time as indicated on the right (n=100 for each group).

(B) Intracellular pH of cells with or without dark foci, cells is derived from 32 hours culture (n=100 for each group).

(C) Cellular ATP concentration of cells with different culture time (at 37°C) as indicated on the bottom.

(D) Cellular ATP concentration of cells treated with different concentrations of CCCP as indicated on the bottom. CCCP were directly added into 12 hours culture and continued to incubate in 37°C shaker for another 4 hours before ATP concentration measurement.

(E) Percentage of cells with IbpA-EGFP foci after 4 hours CCCP treatment. Different concentrations of CCCP were directly added into 12-hour culture and continued to incubate in 37°C shaker for another 4 hours before before observed under a microscope.

(C) to (E) The bars indicate mean of at least three independent experiments; error bar indicates STDEV (*p value < 0.05; **p value < 0.005; ***p value < 0.0005).

(F) Brightfield and fluorescence images showing that protein aggregates are induced by 50 μM CCCP within 4 hours. Protein aggregates labelled by IbpA :: EGFP (left), Lon :: TC-FlAsH (middle) and HslU :: TC-FlAsH (right). The cells were stained with FlAsH for 50 minutes and washed with fresh PBS buffer before CCCP treatment (Scale bar, 2 μm).

See also Figure S4.

Decreased intracellular ATP promotes aggresome formation

Next, we examined the ATP consumption in bacterial cells after long time stationary growth phase culturing with a view to addressing the question of whether this contributed to aggresome formation. Because the current fluorescent ATP sensors for use in single bacterial cells are not reliable after stationary phase culturing (private communication and our own test), we performed population level ATP measurement by using the BacTiter-Glo^{TM} assay which enables extraction of ATP from bacterial cells and utilizes a proprietary thermostable luciferase to support a stable luminescent signal (Conlon et al., 2016). In these experiments, we observed that cellular ATP level decreased significantly in the late stationary phase, where the proportion of insoluble protein with respect to all cellular protein and dormant cell ratio increased notably (Figure 4C, 2B and 1D). The average cellular ATP level at exponential phase (3 hours) is 1.40 ± 0.10 mM, which then increases to 1.53 ± 0.17 mM at mid-stationary phase (12 hours), then decreases sharply to 0.67 ± 0.19 mM after 20 hours culturing and to 0.05 ± 0.01 mM after 32 hours culturing. These observations agree with the previous finding that decreasing the intracellular ATP level by arsenate treatment results in bacterial drug tolerance (Shan et al. 2017), suggesting a strong correlation between ATP depletion and aggresome formation (Figure 4C and 2B).

It is well accepted that ATP is required to maintain proteostasis in a typically highly crowded cytoplasmic environment, as the protein quality control system in

bacterial cells is highly ATP dependent, either for integrated networks of chaperones or for proteases (Baneyx and Mujacic, 2004). More recently, Patel *et al.* proposed that ATP as a biological hydrotrope can directly act to maintain protein solubility and prevent macromolecular aggregation (Patel et al., 2017). To test whether cytosolic ATP depletion would directly induce protein aggresome formation, we used CCCP, a protonophore that can uncouple the proton motive force across the cellular membrane and stop ATP synthase activity, to treat mid-stationary phase cells (12 hours) for an additional 4 hours. As shown in Figure 4D the cellular ATP level decreased in a CCCP concentration dependent manner, in which the intracellular ATP concentration in cells treated with 20 μM CCCP for 4 hours was proximal to the ATP concentration of cells after 32 hours stationary culture. Accordingly, the fraction of cells with protein aggresomes, as assessed by the presence of fluorescent IbpA foci (Figure 4E and S4D), increased with elevated CCCP concentrations. To further confirm that CCCP treatment can induce protein aggresome, we observed the emergence of bright IbpA-EGFP, Lon-TC-FlAsH and HslU-TC-FlAsH foci which colocalised with dark foci in associated brightfield images (Figure 4F) in mid-stationary phase cells (12 hours) treated with CCCP for an additional 4 hours. In contrast, when we returned to our earlier attempt to induce aggresome formation by lowering intracellular pH, we found that adjustment of intracellular pH to 6.92 alone could not induce aggresome formation because the intracellular ATP level of those cells under treatment was not significantly lowered (Figure S4C). Taken together these results suggest that intracellular ATP depletion is the major force driving aggresome formation.

DnaK and ClpB facilitated protein disaggregation is critical for resuscitation of antibiotic tolerant cells

So far, we have established that the presence of protein aggresomes is a strong indicator of bacterial cell dormancy depth, and that intracellular ATP depletion is the major reason driving their formation. Next, we sought to study the molecular mechanism underlying bacterial cell resuscitation. By following the resuscitation course of drug tolerant cells after removing antibiotics, we observed that the dark foci

disappear before dormant cells re-enter the growth cycle, but persist in VBNC cells (Figure 1A). This phenomenon suggests that protein aggresome disaggregation is a critical step for cells to escape dormancy and initiate resuscitation, a process analogous to restoration of proteostasis immediately prior to fertilization in *Caenorhabditis elegans* oocytes (Bohnert and Kenyon, 2017).

Since fresh LB was provided to cells (after stationary culture) during the 6 hours antibiotic killing process and after removing antibiotic the surviving cells were allowed to resuscitate in fresh LB once again, we believe the replenishment of fresh nutrients and hence ATP refill was happening in most surviving cells. However, according to Patel's experiment, if ATP refill alone works to dissolve protein aggregation, its concentration would have to reach a high value (>10 mM) (Patel et al., 2017), almost an order of magnitude higher than the physiological cellular ATP level in bacterial cells (Yaginuma, et al. 2014). Therefore, this reminds us that other biological processes, in addition to ATP refill, are also involved in the clearance of protein aggresomes when cells resuscitate. In *E. coli*, DnaK and ClpB are responsible for dissolving protein aggregates, with DnaK binding directly to the aggregate and recruiting the disaggregase ClpB (Rosenzweig et al., 2013). In the absence of DnaK, ClpB has been shown to have little disaggregation activity, but after directly binding with DnaK, the DnaK-ClpB complex shows high efficiency of disaggregation (Seyffer et al., 2012). We therefore proposed that the DnaK-ClpB bichaperone system also plays a key role in dissolving aggresome to facilitate the regrowth of dormant cells.

To test this hypothesis, we constructed a dual-labelled strain, where Lon was labelled with TC-FlAsH and DnaK with blue fluorescent protein (tagBFP), to observe the dynamics of bacterial protein aggregation and disaggregation during antibiotic treatment and resuscitation. As shown in Figure 5A-C, dormant cells that exhibit both high intensity aggregation and dark foci in brightfield images survived 6 hours of high dosage antibiotic treatment, as anticipated. Surprisingly, in persister cells we found that DnaK was recruited to the aggregate while antibiotic treatment was still ongoing.

Upon removal of the antibiotic, aggregate foci that were packed with DnaK molecules were diminished and cells started to regrow (Figure 5A, Video S3). In stark contrast, in persister-SR cells the protein level of DnaK was initially low with no obvious patterns indicative of aggregate colocalisation, and the cells showed no associated morphological changes. However, as with the persister-FR cells, prior to removal of the antibiotic, cellular DnaK levels increased substantially, colocalising with protein aggregates. Upon removal of antibiotics these protein aggregates dissolved and cell regrowth was initiated on a far longer time scale than in persister-FR cells (Figure 5B, Video S4). In the case of VBNC cells, the cellular DnaK had no visible distinct aggregate-colocalisation pattern; additionally, the protein aggregates and cell morphology showed no obvious transformation during the three days of observation (Figure 5C). We observed similar dynamics in EGFP labelled ClpB during cell resuscitation (Figure S5), confirming that ClpB is part of the DnaK-ClpB apparatus that facilitates protein disaggregation.

To determine the pattern of localization for DnaK foci in cells we labelled DnaK with the photoconvertible fluorescent protein mMaple3 (Wang et al., 2014) for super-resolution imaging. As shown in Figure 5D, DnaK can either form distinct foci, mostly located at cell poles, or distribute evenly throughout the cell. In order to predict the fate of an individual cell we tracked the localisation of DnaK during exposure to the antibiotic and grouped the results according to either uniform (i.e. no detectable foci above the level of background fluorescence) or foci-detected distributions. Our results showed that DnaK foci are more prevalent and more stably coupled with protein aggregates in both persister-SR and persister-FR subgroups than in VBNC cells (Figure 5E) with only about 1/4 of VBNC cells having a transient DnaK foci. These results reveal that protein disaggregation is critical for dormant cells to initiate resuscitation and that DnaK is an important component in this process.
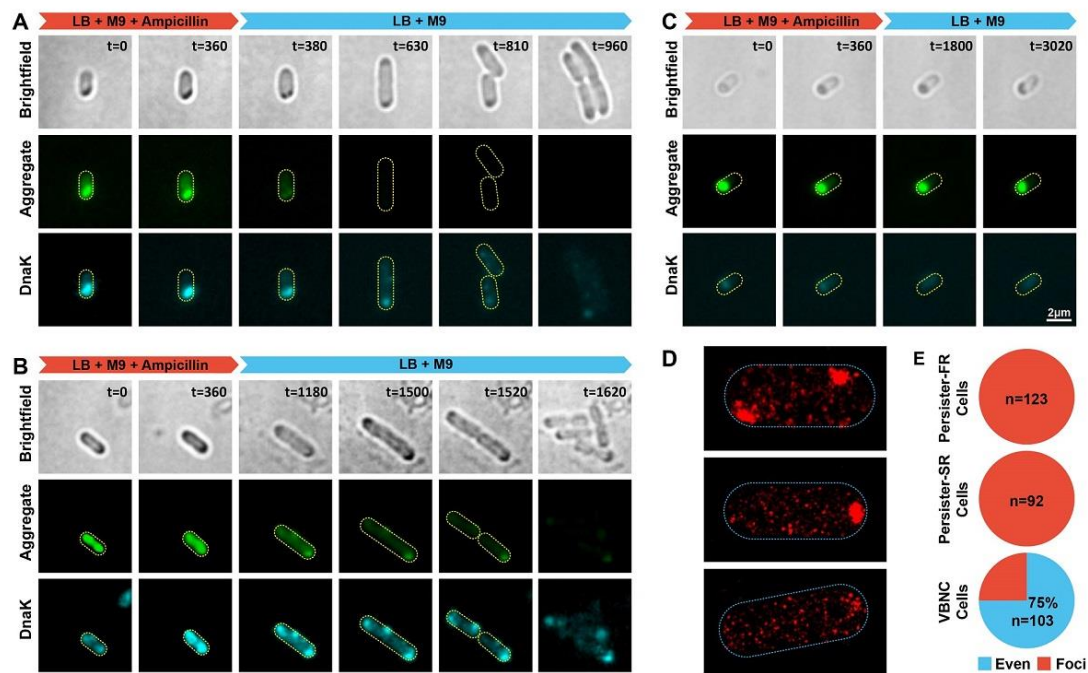
Figure 5. Clearance of protein aggresome and reset of cellular proteostasis before persister cell resuscitation.

(A to C) 24 hours cultured cells of strain DnaK-BFP & Lon-TCtag (in LB) were spotted on a gel-pad and observed under a light microscope. For the antibiotic treatment process, a killing medium was flushed into FCS2 chamber and incubated for 6 hours at 37°C. Then the killing medium was removed by flushing in growth medium (indicated in cyan on the figure) to allow persister cell resuscitation.

(A and B) Time-lapse brightfield and fluorescence images showing aggresome and DnaK :: BFP foci diminish before persister-FR (A) / persister-SR (B) cell resuscitation.

(C) Time-lapse brightfield and fluorescence images showing that protein aggregates remained in VBNC cells, and no visible DnaK :: BFP foci was formed during our observation time. Protein aggresome is visible as dark foci in brightfield images and through Lon :: TC-FlAsH foci in fluorescent images (Scale bar, 2 μm; t=time (min).

(D) Super-resolution images of DnaK :: mMaple3, illustrating DnaK can either form foci or evenly distribute throughout the cell.

(E) Percentage of cells with DnaK :: BFP foci in different cell subgroups, including persister-FR cells, persister-SR cells and VBNC cells.

See also Figure S5.

Dysfunction of the disaggregation machinery generates more dormant cells but less persisters

To further confirm that protein disaggregation is crucial for cell resuscitation we constructed two knockout mutants, *ΔdnaK* and *ΔclpB*, in which dark foci occurred in

brightfield images widely at early stationary phase. As shown in Figure 6B, in comparison with the wild type strain, the dormant cell rate of *ΔdnaK* and *ΔclpB* increased considerably (Figure 6B). Normally with increased dormant cell rate one would expect an increased rate of cell survival after antibiotic treatment as well as an increased persister cell rate. However, we saw an increased rate of cell survival but a decreased resuscitation rate (i.e. a relatively low ratio of persister to all surviving cells), especially in the *ΔdnaK* strain where the resuscitation rate was extremely low (Figure 6C). These results indicate that dormant cells with deficient disaggregation apparatus, regardless of shallow or deep dormancy depth, encounter difficulties in escaping the dormancy trap. This deficient apparatus assists the cells in circumventing the disruptive effect of antibiotics but also prevents them from resuscitation. On the other hand, these results echo our earlier hypothesis that at physiological concentration levels, the hydrotropic activity of ATP alone is not able to facilitate aggresome disintegration.

Previous studies have shown that protein disaggregation by DnaK and ClpB is an ATP-dependent process (Rosenzweig et al., 2013). We constructed two DnaK ATPase activity dysfunctional point mutants, *T199A* and *R261C* (Doyle et al., 2015; Sbai and Alix, 1998). Neither mutant was able to form DnaK foci either after heat shock or in the late stationary phase (Figure 6A), although protein aggregates indicated by dark foci in brightfield images were clearly visible. Compared with the wild type strain, the dormant cell rate of *T199A* and *R261C* increased substantially (Figure 6B), but the resuscitation rate after removal of antibiotic decreased dramatically (Figure 6C). These results indicate that DnaK with impaired ATPase activity is dysfunctional in protein disaggregation, and suggest that the disaggregation machinery itself functions in an ATP-dependent manner.

We have established that heat shock can increase the dormant cell rate through intensified protein aggregation (Figure 3C), which increases cell survival rates and potentially elevates persister rates after antibiotic treatment (Figure 3D). As expected, in the wild type strain the persister rate was substantially increased after heat shock

but in DnaK dysfunctional strains, *T199A* and *R261C,* persister rate was considerably decreased (Figure 6D and S6). These results suggest that intensified protein aggregates deepen dormancy depth, which helps cells evade antibiotic killing and increase the population survival rate but that only cells with functional disaggregation apparatus are capable of efficient resuscitation, the others remaining trapped in a dormant state.
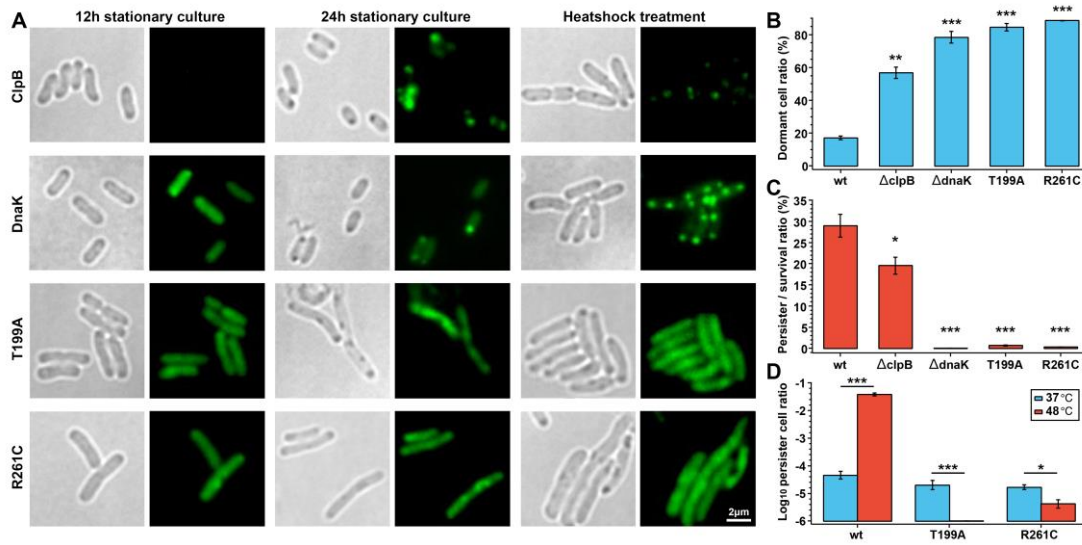

Figure 6. The recruitment of the disaggregation machinery is an ATP-dependent process.
(A) Brightfield and fluorescence images of cells in 12 hours stationary phase (left), 24 hours stationary phase (middle) and heat shock (right) conditions. ClpB :: EGFP and DnaK :: EGFP foci colocalise with protein aggregates in both late stationary and heat shock conditions (upper two panels); ATPase mutants of DnaK, *T199A* and *R261C*, lost the ability to form functional DnaK clusters (lower two panels), (Scale bar, 2 μm).
(B) Dormant cell ratio of cells from different mutants. Dormant cells are defined as cells non-proliferating for at least 6 hours on fresh agarose when observed under a microscope.
(C) Persister cell / survival cell ratio of different mutants. Survival cells were distinguished by live/dead bacterial cell staining; persister cells were the survival cells that subsequently resumed growth in fresh medium.
(D) Frequency of persister formation for different mutant strains without (blue) or with (red) heat shock treatment, determined by antibiotic susceptibility measurement.
(B) to (D) The bars indicate mean of at least three independent experiments; error bar indicates SEM (*p value < 0.05; **p value < 0.005; ***p value < 0.0005).
See also Figure S6.

Discussion

A model for aggresome-regulated bacterial drug tolerance

From our experiments we propose a model to elucidate the aggresome regulated bacterial drug tolerance (Figure 7). In nutrient-depleted *E. coli* cells (i.e. after prolonged stationary phase incubation), cellular ATP is gradually exhausted, leading to proteome-wide protein aggregation and the formation of aggresomes. From mass spectrometry data we find that bacterial aggresomes comprise numerous essential proteins vital for cellular function. Correlated to the appearance of aggresomes, the bacterial cell fails to maintain regular metabolism/proliferation and becomes dormant. With our current analyses it is not possible to determine whether these vital proteins specifically cause aggresomes to form, or whether alternatively some essential proteins enter aggresomes after they have formed – to do so we propose to embark on future dynamic studies of aggresome formation and disintegration to investigate these conflicting hypotheses. Irrespective, this dormant state shields cells from the killing effects of antibiotics. After removal of antibiotic, for a dormant cell to start resuscitation clearance of these aggresomes is a prerequisite. In a nutrient-rich environment, ATP is replenished and DnaK-ClpB protein complexes are recruited to aggresomes, facilitating protein disaggregation. Upon the disaggregation and recovery of proteostasis, the dormant cells are able to resuscitate and regrow. We believe this model has captured the critical steps of aggresome formation and its contribution to bacterial drug tolerance, and provides a useful framework for further exploration of the phenomenon.

An important question which remains unanswered in our study is the destination of the disaggregated peptides after they disassemble from the aggresome. Namely, whether the peptides are refolded and return to their normal cellular function after disaggregation, or they are degraded by the protease machinery to fuel new protein synthesis. We intend to explore these questions in our future studies.

Dormancy depth and lag time

Previously, it has been reported that drug tolerant cells (especially Type I persisters) originate from a minor group of stationary phase cells, which show extremely long lag times. More recently, Fridman *et al.* demonstrated that the lag time of a bacterial population could be modulated through genetic mutations that can be induced by repeated high-dose antibiotic challenges (Fridman et al., 2014). In this work, we propose a new concept termed 'dormancy depth' to measure the degree to which drug tolerant cells are dormant. Although lag time is the direct experimentally measurable quantity, with 'dormancy depth' we are able to provide a unified framework for understanding the formation of both persisters and VBNC cells, and to reveal the molecular origin of lag time. This dormancy depth model has important value in demonstrating that instead of a simple binary active-dormant state, as has been a common assumption, dormancy itself is a heterogeneous physiology state which can be characterized quantitatively as having multiple differing depths. This dormancy depth analysis does not touch directly on the underlying molecular mechanisms of cell resuscitation as such, since the underlying reasons are clearly varied and manifold. However, the concept of dormancy depth does enable robustly quantitative comparisons between the rates of cell recovery under different states of environmental stress even if the underlying molecular mechanisms which bring about their recovery are highly heterogeneous, and importantly creates a solid foundation from which to initiate subsequent mechanistic explorations.

Most importantly, we discover that the extent of aggresome formation is a good indicator of bacterial dormancy depth. Later, from studying the molecular mechanism underlying cell resuscitation, we identify that a cell's ability to disintegrate aggresomes and restore proteostasis is an important but previously unreported factor determining cell fate. Collectively, from the experimental evidence presented in this work, we hypothesize that the relationship between dormancy depth and lag time might be described by lag time = dormancy depth / escaping speed = quantity of aggresomes present / rate of aggresome disaggregation.

Our work represents a major advancement in understanding resuscitation of drug tolerant bacterial cells, by identifying both the key proteins (i.e. those in the DnaK-ClpB complex) and regulatory factors (i.e. intracellular ATP) in this process, the cooperation of which together defines the lag time of drug tolerant cells.

Formation of aggresomes: an active or passive process?

In this work we have discovered dark foci under brightfield microscopy as a transient phenotypic trait of bacterial cells, whose formation is driven by depletion of intracellular ATP. Later, we find that these dark foci comprise with a wide collection of protein aggregates, and thus denote these features as 'aggresomes'. From our work, we may propose that proteins whose solubility is largely influenced by cellular ATP concentration levels are those most prone to precipitate from their solubilized state in the cytosol and aggregate. Of note, it seems such proteome-wide protein aggregation caused by depletion of ATP as a hydrotrope is different from the toxic protein aggregation usually formed by misfolded or unfolded peptides as a result of mutations. Also, in molecular manipulations of bacterial cells (e.g. the expression of fused fluorescent proteins, or expression of plasmids) quite often protein aggregations or inclusion bodies can be observed due to an overexpression of a specific protein. However, these protein aggregations do not result in the phenomenon we report in this study. Therefore, it remains to clarify the physiological state of the proteins included in the bacterial aggresome and to further define the different types of protein aggregation in bacterial cells. Although we have demonstrated that bacterial aggresomes have a functional role in regulating cell dormancy, we cannot draw a conclusion on whether its formation is an active or passive process. It remains to be explored whether cell dormancy through the formation of aggresomes has any active selection advantage over other possible mechanisms.

ATP plays dual roles to maintain cytoplasmic proteostasis

ATP, which is often referred to as the 'molecular unit of currency' for intracellular energy transfer, is one of the most important molecules in all forms of life. It also has other biological functions such as intracellular signaling, materials for

DNA and RNA synthesis, and amino acid activation in protein synthesis. Recently, increasing evidence suggests that ATP plays a critical role in maintaining proteostasis in a typically crowded cytoplasm (Parry, et al. 2014). Our *in vivo* experiments also show that ATP depletion in starved cells causes protein aggresome formation.

ATP is required for the function of protein quality control system, as networks of chaperones and proteases are highly ATP dependent. For example, DnaK plays a central hub role in the network, and requires ATP to fuel its multiple functions in facilitating protein folding and disaggregation. Recently, *in vitro* experiments showed that ATP acts as a biological hydrotrope to maintain protein solubility and prevent macromolecular aggregation (Patel et al., 2017). Rice and Rosen also suggested that the reason why cells maintain mM concentrations of ATP is perhaps to keep proteins soluble by exploiting the hydrotropic activity of ATP, given the Michaelis constant values for ATP-driven cellular processes only require concentrations of between 10-500 μM (Rice and Rosen, 2017). Based on the above analysis, we propose that ATP at physiological concentrations performs dual functions: (i) fuel for protein quality control system; and (ii) also as a hydrotrope, to ensure proteostasis in a crowded cytoplasm.

More on VBNC cells

Colony forming unit (CFU) based viability assays, often used in bacterial antibiotic tolerance studies, lead to negligence of the existence of VBNC cells. Here, based on time-lapse fluorescence microscopy, we establish a bacterial dormancy depth model for a global understanding of bacterial drug tolerance. In this model VBNC cells are in a deeper dormancy depth than persister cells making it more difficult to restore cell physiological conditions and initiate proliferation (Figure 1B). However, the distinction between persister and VBNC cells is not absolute, as demonstrated by our experiments at both single-cell and population levels. Simply by extending the observation time from 1 day to 3 days (Figure 1C), we see the

resuscitation of persister-SR, those of which would be considered to be VBNC cells if the observation time was restricted to 24 hours.

Our model also explains several apparently contradictory results in recent literature, notably studies by Vega *et al.* and Hu *et al.* who show indole can both induce and reduce persister cell formation (Hu et al., 2015; Vega et al., 2012). Increased persister formation from indole may be due to a moderate dormancy depth being induced through the introduction of a stress in the form of indole while decreased persister formation can be attributed to a deep dormancy depth being induced in the cells leading to increased VBNC cell production.

In this paper, we have not explored whether it is possible to awaken VBNC cells by changing the cell culture conditions. In clinical practice, the environment of a bacterial infection site undergoes dynamic and complicated changes, both during and after antibiotic treatment. Therefore, we do not know whether VBNC cells can be awakened by a certain stimuli, which may also lead to disease recurrence. As such we believe VBNC cells should be studied in the same framework with persister cells, and their potential contribution to drug tolerance warrants further studies.

Therapeutic perspective

To tackle bacterial antibiotic tolerance the generally accepted approach is to awaken dormant cells in order to increase antibiotic efficiency (Allison et al., 2011). In contrast, we propose an alternative method of limiting persister production that encourages a bacterium into a deeper state of dormancy to increase the proportion of VBNC cells incapable of resuscitation or regrowth. In our study, we have established that protein aggresomes regulate cell dormancy depth, which is critical for bacterial drug tolerance. As a result, to keep cells in deeper dormancy states we can either aim to intensify protein aggregation to an irreversible level or interrupt disaggregation pathways that prevent cells escaping from their dormant state. Both strategies may present new potential drug targets for the development of future antibiotics.
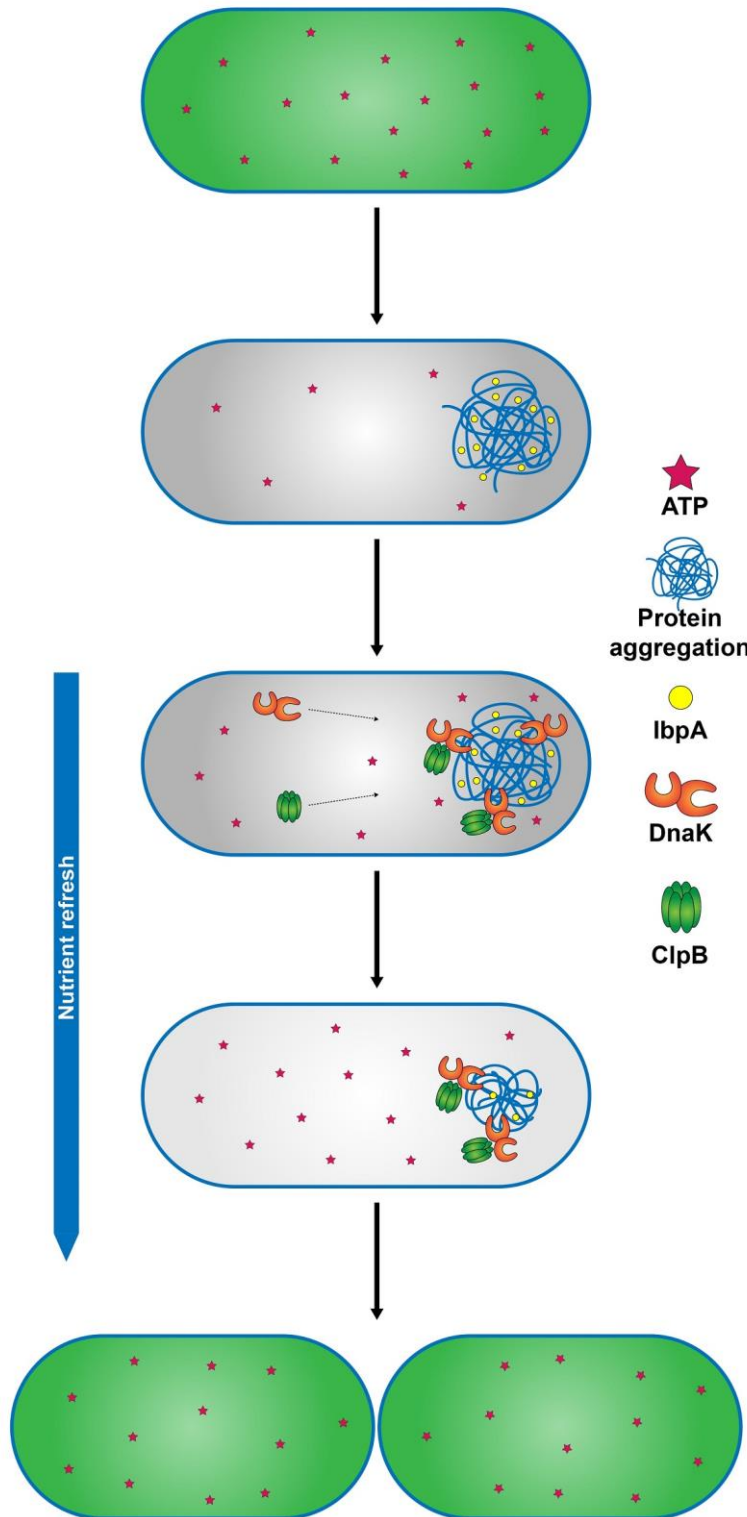
Figure 7. A model for protein aggresome formation and disaggregation in drug tolerant cells.

ACKNOWLEDGMENTS

AUTHOR CONTRIBUTIONS

Conceptualization, Y.P., Y.L., and F.B.; Methodology, Y.P., Y.L., X.J., and T.T.; Investigation, Y.P., Y.L., X.J., T.T., and Z.Z.; Formal Analysis, Y.P., Y.L., Q.M., S.L., Z.C., B.L., G.Y., M.L., and C.L.; Writing - Original Draft, Y.P.; Writing - Review & Editing, M.L. and F.B.; Supervision, F.B.; Funding Acquisition, Y.P., M.L., F.B., and C.L.

DECLARATION OF INTERESTS

The authors declare no competing interests.

References

Allison, K.R., Brynildsen, M.P., and Collins, J.J. (2011). Metabolite-enabled eradication of bacterial persisters by aminoglycosides. Nature *473*, 216-220.

Ayrapetyan, M., Williams, T.C., and Oliver, J.D. (2015). Bridging the gap between viable but non-culturable and antibiotic persistent bacteria. Trends Microbiol *23*, 7-13.

Baba, T., Ara, T., Hasegawa, M., Takai, Y., Okumura, Y., Baba, M., Datsenko, K.A., Tomita, M.,

Wanner, B.L., and Mori, H. (2006). Construction of Escherichia coli K-12 in-frame, single-gene knockout mutants: the Keio collection. Mol Syst Biol *2*, 2006 0008.

Balaban, N.Q., Merrin, J., Chait, R., Kowalik, L., and Leibler, S. (2004). Bacterial persistence as a phenotypic switch. Science *305*, 1622-1625.

Baneyx, F., and Mujacic, M. (2004). Recombinant protein folding and misfolding in Escherichia coli. Nat Biotechnol *22*, 1399-1408.

Bohnert, K.A., and Kenyon, C. (2017). A lysosomal switch triggers proteostasis renewal in the immortal C. elegans germ lineage. Nature *551*, 629-633.

Boucher, R.C. (2001). Pathogenesis of cystic fibrosis airways disease. Trans Am Clin Climatol Assoc *112*, 99-107.

Chao, M.C., and Rubin, E.J. (2010). Letting sleeping dos lie: does dormancy play a role in tuberculosis? Annu Rev Microbiol *64*, 293-311.

Conlon, B.P., Rowe, S.E., Gandt, A.B., Nuxoll, A.S., Donegan, N.P., Zalis, E.A., Clair, G., Adkins, J.N., Cheung, A.L., and Lewis, K. (2016). Persister formation in Staphylococcus aureus is associated with ATP depletion. Nat Microbiol *1*, 16051.

Datta, S., Costantino, N., and Court, D.L. (2006). A set of recombineering plasmids for gram-negative bacteria. Gene *379*, 109-115.

Datsenko, K.A., and Wanner, B.L. (2000). One-step inactivation of chromosomal genes in Escherichia coli K-12 using PCR products. Proc Natl Acad Sci U S A *97*, 6640-6645.

Fridman, O., Goldberg, A., Ronin, I., Shoresh, N., and Balaban, N.Q. (2014). Optimization of lag time underlies antibiotic tolerance in evolved bacterial populations. Nature *513*, 418-421.

Giacalone, M.J., Gentile, A.M., Lovitt, B.T., Berkley, N.L., Gunderson, C.W., and Surber, M.W. (2006). Toxic protein expression in Escherichia coli using a rhamnose-based tightly regulated and tunable promoter system. Biotechniques *40*, 355-364.

Hansen, S., Lewis, K., and Vulic, M. (2008). Role of global regulators and nucleotide metabolism in antibiotic tolerance in Escherichia coli. Antimicrob Agents Chemother *52*, 2718-2726.

Harshman, R.B., and Yamazaki, H. (1971). Formation of ppGpp in a relaxed and stringent strain of Escherichia coli during diauxie lag. Biochemistry *10*, 3980-3982.

Hartl, F.U., Bracher, A., and Hayer-Hartl, M. (2011). Molecular chaperones in protein folding and proteostasis. Nature *475*, 324-332.

Hu, Y., Kwan, B.W., Osbourne, D.O., Benedik, M.J., and Wood, T.K. (2015). Toxin YafQ increases persister cell formation by reducing indole signalling. Environ Microbiol *17*, 1275-1285.

Huang, B., Wang, W., Bates, M., and Zhuang, X. (2008). Three-dimensional super-resolution imaging by stochastic optical reconstruction microscopy. Science *319*, 810-813.

Ignatova, Z., and Gierasch, L.M. (2004). Monitoring protein stability and aggregation in vivo by real-time fluorescent labeling. Proc Natl Acad Sci U S A *101*, 523-528.

Kaspy, I., Rotem, E., Weiss, N., Ronin, I., Balaban, N.Q., and Glaser, G. (2013). HipA-mediated antibiotic persistence via phosphorylation of the glutamyl-tRNA-synthetase. Nature Communications *4*.

Krasnopeeva, K., Lo, C.J., Pilizota, T. (2018) Revealing the mechanisms of stress induced damage through free energy dynamics analysis. http://arxiv.org/abs/1809.05306

Lindner, A.B., Madden, R., Demarez, A., Stewart, E.J., and Taddei, F. (2008). Asymmetric segregation of protein aggregates is associated with cellular aging and rejuvenation. Proc Natl Acad Sci U S A *105*, 3076-3081.

Martinez, K.A., 2nd, Kitko, R.D., Mershon, J.P., Adcox, H.E., Malek, K.A., Berkmen, M.B., and Slonczewski, J.L. (2012). Cytoplasmic pH response to acid stress in individual cells of Escherichia coli and Bacillus subtilis observed by fluorescence ratio imaging microscopy. Appl Environ Microbiol 78, 3706-3714.

Miesenbock, G., De Angelis, D.A., and Rothman, J.E. (1998). Visualizing secretion and synaptic transmission with pH-sensitive green fluorescent proteins. Nature 394, 192-195.

Mirzaei, H., and Regnier, F. (2008). Protein:protein aggregation induced by protein oxidation. J Chromatogr B Analyt Technol Biomed Life Sci 873, 8-14.

Moyed, H.S., and Bertrand, K.P. (1983). hipA, a newly recognized gene of Escherichia coli K-12 that affects frequency of persistence after inhibition of murein synthesis. J Bacteriol 155, 768-775.

Olsen, J.V., Ong, S.E., and Mann, M. (2004). Trypsin cleaves exclusively C-terminal to arginine and lysine residues. Mol Cell Proteomics 3, 608-614.

Parry, B.R., Surovtsev, I.V., Cabeen, M.T., O'Hern, C.S., Dufresne, E.R., and Jacobs-Wagner, C. (2014). The bacterial cytoplasm has glass-like properties and is fluidized by metabolic activity. Cell 156, 183-194.

Patel, A., Malinovska, L., Saha, S., Wang, J., Alberti, S., Krishnan, Y., and Hyman, A.A. (2017). ATP as a biological hydrotrope. Science 356, 753-756.

Pu, Y., Zhao, Z., Li, Y., Zou, J., Ma, Q., Zhao, Y., Ke, Y., Zhu, Y., Chen, H., Baker, M.A., et al. (2016). Enhanced Efflux Activity Facilitates Drug Tolerance in Dormant Bacterial Cells. Mol Cell 62, 284-294.

Rosenzweig, R., Moradi, S., Zarrine-Afsar, A., Glover, J.R., and Kay, L.E. (2013). Unraveling the mechanism of protein disaggregation through a ClpB-DnaK interaction. Science 339, 1080-1083.

Sbai, M., and Alix, J.H. (1998). DnaK-dependent ribosome biogenesis in Escherichia coli: competition for dominance between the alleles dnaK756 and dnaK+. Mol Gen Genet 260, 199-206.

Seyffer, F., Kummer, E., Oguchi, Y., Winkler, J., Kumar, M., Zahn, R., Sourjik, V., Bukau, B., and Mogk, A. (2012). Hsp70 proteins bind Hsp100 regulatory M domains to activate AAA+ disaggregase at aggregate surfaces. Nat Struct Mol Biol 19, 1347-1355.

Shan, Y., Brown Gandt, A., Rowe, S.E., Deisinger, J.P., Conlon, B.P., and Lewis, K. (2017). ATP-Dependent Persister Formation in Escherichia coli. MBio 8(1):e02267-16

Siibak, T., Peil, L., Xiong, L.Q., Mankin, A., Remme, J., and Tenson, T. (2009). Erythromycin- and Chloramphenicol-Induced Ribosomal Assembly Defects Are Secondary Effects of Protein Synthesis Inhibition. Antimicrob Agents Ch 53, 563-571.

Tomoyasu, T., Mogk, A., Langen, H., Goloubinoff, P., and Bukau, B. (2001). Genetic dissection of the roles of chaperones and proteases in protein folding and degradation in the Escherichia coli cytosol. Mol Microbiol 40, 397-413.

Toprak, E., Veres, A., Michel, J.B., Chait, R., Hartl, D.L., and Kishony, R. (2011). Evolutionary paths to antibiotic resistance under dynamically sustained drug selection. Nat Genet 44, 101-105.

Ungelenk, S., Moayed, F., Ho, C.T., Grousl, T., Scharf, A., Mashaghi, A., Tans, S., Mayer, M.P., Mogk, A., and Bukau, B. (2016). Small heat shock proteins sequester misfolding proteins in near-native conformation for cellular protection and efficient refolding. Nat Commun 7, 13673.

Vega, N.M., Allison, K.R., Khalil, A.S., and Collins, J.J. (2012). Signaling-mediated bacterial persister formation. Nat Chem Biol 8, 431-433.

Wallace, E.W., Kear-Scott, J.L., Pilipenko, E.V., Schwartz, M.H., Laskowski, P.R., Rojek, A.E., Katanski, C.D., Riback, J.A., Dion, M.F., Franks, A.M., et al. (2015). Reversible, specific, active aggregates of endogenous proteins assemble upon heat stress. Cell 162, 1286-1298.

Wang, S., Moffitt, J.R., Dempsey, G.T., Xie, X.S., and Zhuang, X. (2014). Characterization and development of photoactivatable fluorescent proteins for single-molecule-based superresolution imaging. Proc Natl Acad Sci U S A *111*, 8452-8457.

Wang, X., Fujimaki, K., Mitchell, G.C., Kwon, J.S., Della Croce, K., Langsdorf, C., Zhang, H.H., and Yao, G. (2017). Exit from quiescence displays a memory of cell growth and division. Nat Commun *8*, 321.

Winkler, J., Seybert, A., Konig, L., Pruggnaller, S., Haselmann, U., Sourjik, V., Weiss, M., Frangakis, A.S., Mogk, A., and Bukau, B. (2010). Quantitative and spatio-temporal features of protein aggregation in Escherichia coli and consequences on protein quality control and cellular ageing. EMBO J *29*, 910-923.

Yaginuma, H., Kawai, S., Tabata, K.V., Tomiyama, K., Kakizuka, A., Komatsuzaki, T., Noji, H., and Imamura, H. (2014). Diversity in ATP concentrations in a single bacterial cell population revealed by quantitative single-cell imaging. Sci Rep 4, 6522.

Zhou, C., Slaughter, B.D., Unruh, J.R., Guo, F., Yu, Z., Mickey, K., Narkar, A., Ross, R.T., McClain, M., and Li, R. (2014). Organelle-based aggregation and retention of damaged proteins in asymmetrically dividing cells. Cell *159*, 530-542.

STAR Methods

CONTACT FOR REAGENT AND RESOURCE SHARING

Further information and requests for resources and reagents should be directed to and will be fulfilled by the Lead Contact, Fan Bai (fbai@pku.edu.cn).

EXPERIMENTAL MODEL AND SUBJECT DETAILS

Bacterial Strains

E. coli strains MG1655, BW25113, *lon-TCtag, hslU-TCtag, EK07, IbpA-EGFP, dnaK-EGFP, clpB-EGFP, DnaK-BFP & Lon-Tctag, DnaK-mMaple3, T199A* and *R261C* were grown in Luria Broth (LB); strains *ΔclpB* and *ΔdnaK* were cultured in LB with 50 mg/mL kanamycin.

METHOD DETAILS

Bacterial strains construction, related to Figure S7

Strains containing target chromosomal gene -fluorescent protein (FP) translational fusion or single target gene knockout mutants were constructed by λ-red mediated gene replacement. For fluorescent protein fusion strains (Datsenko and Wanner, 2000): the targeted fluorescent protein (EGFP, TagBFP, or mMaple3) fragment was amplified and inserted to replace the stop cassette of the selection-counter-selection template plasmid (pSCS3V31C). Then the linker-FP-Toxin-CmR fragment was amplified from the template plasmid with homology arm complementary to the flanking sequences of the insertion site on the chromosome, before being transformed into electrocompetent cells with induced recombineering helper plasmid (pSIM6) (Datta, et al. 2006). After 3-5 hours recovery, transformed cells were plated on selection plates containing chloramphenicol. The Toxin-CmR cassette was then removed from the chromosome by another round of λ red mediated recombination using a counter selection template. Finally, cells were plated on counter selection plates containing rhamnose to activate toxin (Giacalone et al., 2006).

For TC-tag (CCPGCC) strains and point mutation strains we amplified the Toxin-CmR cassette

from pSCS3V31C to insert into the TC-tag or point mutation target site on the chromosome. The counter selection template containing TC-tag/mutation sequence and flanking chromosome sequence as the homologous arm was used to replace the Toxin-CmR cassette with the TC-tag/mutation sequence. Lon-TCtag and hslU-TCtag strains were obtained by inserting the TC-tag into amino acid position 731 of Lon and position 363 of HslU. Dnak point mutants T199A and R261C were modified from the DnaK-EGFP strain, in which wild type DnaK with amino acid mutations T→A at position 199 and R→C at position 261, respectively. For *ΔdnaK* strain, we used the Keio cassette flanked by FRT sites in the Keio collection to replace the *dnaK* gene on the chromosome. All primers we have used are listed in Table S2.

Cell staining for Fluorescence microscopy

For FlAsH staining (Ignatova and Gierasch, 2004), cells were harvested and washed three times with PBS and treated with 10 mM EDTA for 15 minutes to improve membrane permeability. Cells were then re-suspended in PBS buffer supplemented with 8 μM FlAsH-EDT2 (Invitrogen) and incubated for 50 minutes in the dark at 37°C. The FlAsH-EDT2 was washed away before heat shock or CCCP treatment.

For Propidium iodide (PI) staining, cells were stained with PI dye (Invitrogen Molecular Probes' LIVE/DEAD *Bac*Light Bacterial Viability Kits) at a final concentration of 40 μM (according to Manufactur's instruction). The cells were incubated for 15 minutes protected from light at room temperature in order to distinguish dead from surviving cells. The camera exposure time and gain were adjusted to prevent over-saturated image acquisition.

Brightfield and Fluorescence microscopy

Brightfield and fluorescence imaging were performed on an inverted microscope (Zeiss Observer.Z1). Illumination was provided by different solid state lasers (Coherent), at wavelengths 405 nm for TagBFP, 488 nm for FlAsH and EGFP, and 561 nm for propidium iodide (PI). The fluorescence emission signal of cells was imaged onto an EMCCD camera (Photometrics Evolve 512). Appropriate filter sets were selected for each fluorophore according to their excitation and emission spectra.

Time-lapse recording of antibiotic killing and bacteria resuscitation under a microscope

For prolonged bacterial culturing and time-lapse imaging we used the Flow Cell System FCS2 (Bioptechs) (Pu et al., 2016). Cells cultured overnight were collected, washed three times with M9 minimal medium and imaged on a gel-pad containing 2% low melting temperature agarose (volume of cell culture: volume of gel-pad = 1: 20). The gel-pad was prepared in the center of the FCS2 chamber as a gel island and surrounded by flowing medium buffer with different ingredients according to experimental requirements (as shown in figure legends for each set of time-lapse experiment). The cells were then observed under brightfield/epifluorescence illumination at 37°C.

To record the antibiotic-mediated killing and bacterial resuscitation under a light microscope bacterial cells were exposed to 150 μg/ml ampicillin in 90% M9 + 10% LB medium for 6 hours at 37°C and then fresh growth medium 90% M9 + 10% LB was flushed in. The growth medium was refreshed every 12 hours, allowing cells to recover sufficiently.

Dormant cell ratio and persister/survival ratio determination

LB cultured cells taken from the indicated time points were collected, washed three times with M9 minimal medium and placed on a fresh gel-pad in FCS2 system as described above. To record bacterial resuscitation under a light microscope we followed the procedure described above.

For dormant cell ratio analysis the samples were spotted on a gel-pad after PI dye staining to exclude dead cells and their growth was recorded by time-lapse imaging. Dormant cells were defined as cells non-proliferating for at least 6 hours on a fresh gel-pad when observed under a microscope. For persister/surviving cell ratio analysis, after 5 hours ampicillin killing in a 37°C shaker, cells were washed to remove antibiotics and stained with PI dye. The cells were observed on a gel-pad to record their recovery under the microscope. Survival cells were distinguished by live/dead bacterial cell staining; persister cells were the survival cells that resumed growth in fresh medium.

Antibiotic treatment and persister counting assay

Bacterial cultures were diluted by 1:20 into fresh LB containing 150 μg/mL ampicillin and incubated in a shaker (200rpm) for 5 hours at 37°C. Samples were then removed, diluted serially in PBS buffer and spotted on LB agar plates for overnight culturing at 37°C. Colony formation unit (CFU) counting was performed the next day. Extended CFU counting was performed daily for 5 days. CFU experiments were performed in triplicate.

Heat shock experiment

For the persister counting assay after heat shock treatment the 16 hours overnight culture was transferred to 1.5 mL tubes and incubated on a dry bath at different temperatures (42°C to 50°C) for 60 minutes. After heat shock treatment samples were grown on an LB agarose gel-pad under the microscope for the dormant ratio assay or were diluted by 1:20 into fresh LB with 150 μg/mL ampicillin for persister counting assay.

Chloramphenicol treatment

Cells cultured in LB for 16 hours at 37°C were taken out and split into two tubes, one treated with 25 μg/ml chloramphenicol and the other set as control. Then the tubes were returned to the incubator for further culture. Next, a fraction of cells was collected at indicated time points (16h, 24h, 32h) and washed away chloramphenicol with fresh LB for dormant cell ratio analysis on an agarose gel-pad or persister counting assay after ampicillin treatment.

The measurement of cellular pH

Intracellular cytoplasmic pH was determined by using a constitutively expressing ratiometric pHluorin (strain EK07) through measuring the 405/488-nm excitation ratios and converting to pH values based on a calibration curve (Figure S1G). The calibration curve was generated by measurement of the 405/488-nm excitation ratios of purified pHluorin at different pH values as described previously (Miesenbock et al., 1998 and Krasnopeeva et al., 2018). Briefly, fluorescence excitation spectra from purified pHluorin in buffers of defined pH were recorded under a light microscope, and the 405-/488-nm excitation ratios of pHluorin fluorescence intensities were determined at different pH values to generate a calibration curve.

The measurement of cellular ATP

ATP levels of the cultures with different culture times or with the addition of various concentration of CCCP treatment were measured using BacTiter-Glo[TM] Microbial Cell Viability Assay (Promega, G8231) following the manufacturer's instructions (Conlon et al., 2016). Intracellular ATP concentration was determined through normalizing ATP levels by cell number and single cell volume. Different concentrations of CCCP were added to treat cells for 4 hours before ATP measurement or observation under a microscope.

Super-resolution fluorescence microscopy

Sample preparation, image processing and data analysis was modified from Huang (Huang et al., 2008). Strain DnaK-mMaple3 was cultured overnight in 4 ml LB at 37°C. Cells were harvested by centrifugation at 5000g for 2 minutes and washed with filtered PBS 3 times. Cells were then fixed with 4% PFA for 15 minutes and washed with PBS another 3 times to remove residual PFA. The fixed cells were inserted into a poly-l-lysine coated flow chamber, incubated for 20 minutes at room temperature and washed with approximately 150 μl (10 times chamber volume) of PBS to remove extra cells. To calibrate for stage drift during data acquisition, 100 nm Tetraspeck beads (Invitrogen, T-7279, 1:10,000 in PBS) were added to the sample before the chamber was sealed with nail polish.

Cells were imaged using TIRF illumination mode on a custom-built STochastic Optical Reconstruction Microscopy (STORM) imaging platform based on an Olympus 83 microscope. Three sets of data for each field of view were collected: brightfield, conventional fluorescence (488 nm Excitation) and super-resolution fluorescence (561 nm Excitation). For both brightfield and conventional fluorescence 10 frames were collected and the images were averaged. Super-resolution images were acquired by continuous illumination from a 561 nm wavelength laser with a power density of $2kW/cm^2$ at a frame rate of 60 Hz and the intensity of the 405 nm wavelength laser was increased stepwise for optimal photoconversion rates during data acquisition. Imaging of each field was performed until all mMaple3 molecules were completely bleached.

Insoluble protein isolation and SDS-PAGE

The method for insoluble protein isolation from bacterial cells was modified from Tomoyasu (Tomoyasu et al., 2001). Aliquots of bacterial cultures with the same optical density (2 ml of culture of $OD_{600}=1$) were rapidly cooled on ice to 0°C. Cultures were then centrifuged at 5000g (4°C) for 10 minutes to harvest the cells. Pellets were suspended in 40 μl buffer A (10mM potassium phosphate buffer, pH 6.5, 1 mM EDTA, 20% (w/v) sucrose, 1 mg/ml lysozyme) and incubated for 30 minutes on ice. Cell lysate was combined with 360 μl of buffer B (10mM potassium phosphate buffer, pH 6.5, 1 mM EDTA) and sonication while cooling. The pellet fractions were resuspended in 400 μl of buffer C (buffer B with 2% NP40) to dissolve membrane proteins and the aggregated proteins were isolated by centrifugation 15 000 g, 30 minutes, 4°C. NP40-insoluble pellets were washed twice with 400 μl of buffer B and re-suspended in 50 μl of buffer B by brief sonication.

Gel electrophoresis of the aggregated protein was carried out using 12% SDS ± PAGE and staining with Coomassie brilliant blue.

Mass spectrometry

For protein identification, the Coomassie-stained total aggregated proteins of each sample were cut out of the gel and destained with a solution of 100 mM ammonium bicarbonate in 50% acetonitrile. After dithiothreitol reduction and iodoacetamide alkylation the proteins were digested with porcine trypsin (Sequencing grade modified; Promega, Madison, WI) overnight at 37 °C (Olsen et al., 2004). The resulting tryptic peptides were extracted from the gel pieces with 80% acetonitrile, 0.1% formic acid (FA). The samples were dried in a vacuum centrifuge concentrator at 30 °C and resuspended in 10 μl 0.1%FA.

Using an Easy-nLC 1200 system, 5 μl of sample was loaded at a speed of 0.3 μl/min in 0.1% FA onto a trap column (C$_{18}$, Acclaim PepMap ^{TM} 100 75μm x 2cm nanoViper Thermo) and eluted across a fritless analytical resolving column (C$_{18}$, Acclaim PepMap ^{TM} 75 μm x15cm nanoViper RSLC Thermo) with a 75 minutes gradient of 4% to 30% LC-MS buffer B (LC-MS buffer A includes 0.1% formic acid; LC-MS buffer B includes 0.1% formic acid and 80% ACN) at 300 nl/min.

Peptides were directly injected into a Thermo Orbitrap Fusion Lumos using a nano-electrospray ion source with electrospray voltages of 2.1 kV. Full scan MS spectra were acquired in the Orbitrap mass analyzer (m/z range: 300–1500 Da) with the resolution set to 120,000 (FWHM) at m/z 200 Da. Full scan target was 1x10^6 with a maximum fill time of 50 ms. All data were acquired in profile mode using positive polarity. MS spectra data were acquired in the Orbitrap with a resolution of 30,000 (FWHM) at m/z 200 Da and higher-collisional dissociation (HCD) MS fragmentation.

QUANTIFICATION AND STATISTICAL ANALYSIS

Image analysis and statistics.

For the time-lapse fluorescence imaging experiments, the fate of different bacterial cells after treatment with antibiotic was determined. Subsequently, by tracing the pattern and intensity of their fluorescence signal during and after antibiotic treatment we determined the relationship between these characteristics and the cell fate.

Image analysis was performed using ImageJ software (Fiji). Outlines of cells were identified from brightfield images. Pixel intensity of all pixels within a cell were measured from the fluorescence emission channel after subtraction of background and autofluorescence. From the resulting individual cell intensity histograms, we consider pixel fluorescence intensity (f) above the mean fluorescent intensity of the cell (a), and assign them to foci if f>2a, and if more than four such pixels were adjacent to each other.

Super-resolution fluorescence microscopy data analysis

Super-resolution fluorescence microscopy data was analyzed following the protocol previously described by Huang *et al.* in 2008 (Huang et al., 2008).

Mass spectrometry data analysis

The MS data were aligned with *Escherichia coli* Reviewed Swiss-Port database by Proteome Discoverer 2.1 software. The mass spectrometry proteomics data have been deposited to the ProteomeXchange Consortium via the PRIDE partner repository with the dataset identifier PXD011288 and 10.6019/PXD011288

Supplemental item titles and legends

Video S1. Time-lapse microscopy showing protein aggregates in persister-FR cells dissolved gradually before resuscitation. Related to Figure 1A.

Cell culture from stationary phase was placed on a gel-pad then treated for 360 minutes with 150 μg/ml of ampicillin in medium (90% (v/v) M9 + 10% (v/v) LB medium). During this period, brightfield and fluorescent images were acquired automatically every 15 minutes at an exposure time of 100 ms. At t=360 minutes fresh medium (90% (v/v) M9 + 10% (v/v) LB medium) was injected to remove antibiotic allowing surviving cells to resume growth. Images were captured automatically every 20 minutes at an exposure time of 100 ms. Samples were maintained at 37°C for the duration of the experiment.

Video S2. Time-lapse microscopy showing protein aggregates in persister-SR cells dissolved gradually before resuscitation. Related to Figure 1A.

Description identical to that of Video S1.

Video S3. Time-lapse microscopy showing protein aggregates in persister-FR cells dissolved gradually before resuscitation. Related to Figure 5A.

Description identical to that of Video S1.

Video S4. Time-lapse microscopy showing protein aggregates in persister-SR cells dissolved gradually before resuscitation. Related to Figure 5B.

Description identical to that of Video S1.

Table S1. Total insoluble protein mass-spectrometric analysis. Related to Figure 2 and Figure 3.

Table S2. All the primers used in this study. Related to STAR Methods.